

Evaluation of Rain Cell Size Distribution Pattern on Signal Transmission.

Ebinowen Tusin Dayo¹ and Adeshina Sirajdin Olagoke²

¹School of Electrical and Electronic Engineering, Universiti Sains Malaysia, 14300 Nibong Tebal, Penang, Malaysia

ABSTRACT

Rain fade is the most common propagation problem at Ku-band frequencies and above, especially in tropical places where rainy seasons outnumber dry seasons. Due to the multiple applications of satellite communication in this band, higher frequencies have broader bandwidth and channel capacity performance. Due to its shorter wavelength of 2.5 cm - 1.67 cm compared to average rain cell sizes, the Ku band operates at a frequency spectrum above 10 GHz and is strongly affected by rain-fade. Because of the unpredictable weather in this region, other researchers' models were based on a different season of the year, however this research was conducted on an annual basis and was fitted with an assumption based on Excel application, and it also offered parametric fits using MATLAB, which is a relatively new technology. Above all, more recent data were employed in this study's analysis. The effect of the rain cell size distribution pattern on signal transmission in the Ku band was investigated in this research. For the estimation of site diversity and improvement factor needed to evaluate the size of the rain cell pattern, rain data from three different rain locations (A, B, C) were archived for two years between 2012 and 2014 within a system that covered the study of raindrop cell size and its effect on signal propagation at the referenced band.

KEYWORDS: Rainfade, Ku-band, bandwidth, wavelength, Raindrop

Date of Submission: 24-07-2021

Date of acceptance: 09-08-2021

I. INTRODUCTION

Components in the troposphere, which stretches from the Earth's surface to heights of roughly 10 km to 20 km vertically extended in the temperate and tropic areas, are the primary cause of radio wave signal propagation impairments above 10 GHz. Frequencies below 10 GHz are frequently affected by ionosphere degradation (50-100 km). At frequencies over 10 GHz, the ionosphere is essentially transparent to radio waves [9]. In terms of quality and availability objectives, however, links propagated over higher frequency bands (above 10 GHz) suffer significant damage due to rain fading [6], [7], and others. Apart from hydrometeor absorption, gaseous absorption, primarily from oxygen and water vapour, contributes to overall radio wave attenuation, particularly at low elevation angles. However, as compared to the attenuation caused by rain, the contribution of gaseous absorption to total attenuation is minor. The presence of hydrometeors in the propagation route, particularly rain, causes dispersion and absorption of radio waves. To the incident wave, raindrops act as dissipative dielectric media. To the incident wave, raindrops act as dissipative dielectric media. The scattering is linked to changes in wave propagation directions in order to meet boundary conditions at raindrop surfaces. Attenuation is caused by the interaction of these two processes, which is dependent on the conductivity and form of the drops. Rainfall attenuation is a critical factor in the design of Earth-satellite radio communications operating at frequencies above 10 GHz. Rain fade of radio waves, which affects satellite communications signals with frequencies higher than 10 GHz, such as Ku band (18/12 GHz), Ka band (30/20 GHz), and V band (50/40 GHz), is widely recognised [2]. In heavy rain places like the tropics, rain attenuation can be very severe, even for Ku-band radio waves [11], [12]. Rain drop results in a reduction of signal intensity at the receiver, as well as a waste of transmission power in an attempt to overcome this type of attenuation. In extreme instances, there may be no signal at all at the receiver, and the satellite link may be unavailable for a greater percentage of the time [13]. With the growing use of satellite communication systems around the world, It becomes vital to investigate microwave attenuation by precipitation in a variety of climate zones. Although

rain is the most major hydrometeor affecting radio wave propagation, clouds, fog, hail, and snow can all have an impact on a radio wave's passage through space. The formation of clouds is linked to the formation of rain. Clouds are visible aggregation of minute droplets of water or microscopic crystals of ice particles, and they are a type of condensation. Three basic cloud forms will be described in this book. Cirrus, Cumulus, and Stratus clouds are the three types of clouds. Cirrus clouds are tall, white, and slender clouds. They split or detach, forming fragile veil-like patches or extended wispy fiber with a feathery appearance. Individual globular masses make up a cumulus cloud. Stratus clouds are best described as sheets or layers that cover much or all of the sky, and they usually have a flat foundation and the appearance of rising domes or towers. Although there may be tiny breaks, as shown in Figure 2.1, there are no distinguishable individual cloud units.



Cirrus radiatus

(a)



Stratus

(b)



(c)

Typical representations of (a) Cirrus cloud, (b) Stratus cloud, and (c) Cumulus cloud are shown in Figure 2.1.

When characterizing the heights at which cloud bases occur, a long-established sub-division of the troposphere into three layers – low, medium, and high – is still utilized [8]. Refractive processes are not lossy, but rather redistribute radio wave energy arriving at an antenna over time, resulting in fading as well as an increase in received power. The principal refractive process for elevation angles greater than 10° is tropospheric

scintillation, which is caused by scattering from small-scale refractive index inhomogeneities along the path. Large-scale multipath can cause severe “low-angle fading,” as well as beam defocusing caused by the vertical gradient of atmospheric refractivity, on pathways with elevation angles below 5° . For satellite multimedia service delivery and quality-of-service (QoS) issues, the corresponding propagation delays and fluctuations are critical [3]. When a radio signal travels through the atmosphere, it experiences attenuation. Rain fades, which are the most common problem, are mainly caused by rain [10]. Water molecules in a rain droplet absorb part or all of the signal energy of a passing radio wave with a shorter wavelength than water molecule sizes, according to [5].

II. METHODOLOGY

TRODAN was created to create a data bank of measured parameters for an observatory, for research, and as a tool for planning appropriate terrestrial and satellite communication networks, to name a few applications. Campbell Scientific Automatic Weather Station provided the data for this study. The apparatus also measured relative humidity, soil temperature, air temperature, wind speed, wind direction, barometric pressure, volumetric water content, sun radiation, and rainfall amount, among other meteorological characteristics. The TRODAN observatory and a typical rain gauge are shown in Figures 3.2 and 3.3, respectively. The rain rate measurements were taken with a tipping bucket rain gauge, which stands at 146 mm in height. The rain gauge has a 400 cm² aperture with a resolution and efficacy of 0.2 mm per tip. Rainwater was gathered in a conventional funnel and split into equal-sized drips. Every 10 seconds, the quantity of drips collected was electronically counted and then averaged over 5 minutes. During this observation, continuous 5-minute averaged rainfall rates were observed, logged, and later downloaded to the computer. The data was recorded at 5-minute intervals for a total of 24 hours. The 5-minute rainfall data was transformed to 1-minute integration data using the approach of Lavergnant and Gole since [4] proved that 1-minute integration time is adequate for attenuation prediction for frequencies greater than 10 GHz (1998). The model is ideal for this research because it has the advantage of translating both the probability of rain rate occurring in 5-minute integration time to the likelihood of rain rate occurring in 1-minute as well as converting the equivalent rain rate of 5-minute to 1-minute. This method was created as a stochastic process application for the time intervals between raindrops and has a solid theoretical foundation. This approach has the advantage of allowing conversion between any integration times. The data from the TRODAN site was simulated in Simulink software using MATLAB.

Equations (3.1) and (3.2) show the rain rate for a 1-minute integration period as well as the percentage of time the rain rate is prolonged for a 1-minute integration time.

$$R_1 = \frac{R_5}{CF} \quad (3.1)$$

$$P_1(R_1) = CF P_5(R_5) \quad (3.2)$$

where,

R_1 represents the rain rate for a 1-minute integration time, P_1 represents the percentage of time the rain rate was exceeded for a 1-minute integration time, R_5 represents the rain rate for a 5-minute integration time, P_5 represents the percentage of time the rain rate was exceeded for a 5-minute integration time, and CF represents the conversion factor.



TRODAN observatory Garden at FUTA, Nigeria (Figure 3.2).



Figure 3.3: The TRODAN observatory garden at FUTA uses a tipping bucket rain gauge.

III. RESULTS AND DISCUSSION

The header text lines in all files have twelve rows, each of which begins with a date/time in the same cell in the format ddmmYYYYhhmm. The second row contains the CR 1000 record, which is the data logger type used for data collection, the third row contains the CR 1000 Battery Volt, and the fourth row contains the meteorological parameters, which begin with Rain Rate in mm, Solar Radiation SLrW in W/m², Air Temperature AirTC in Degree Celsius (°C), Rain rate in mm/hr., Relative Humidity RH in Percentage (percent), Soil Temperature T107 in °C Barometric Pressure Barpress in mbar, Volumetric Water Content VW *100, Wind Direction in Degrees Finally, PA is used for unified soil conversion, which solely concerns volumetric water content. The data's serial number is stored in this column. Product name, creation time, units, source, missing data, end of record identifier, and time range are all included in the header. Barometric Pressure Barpress in mbar, Volumetric Water Content VW *100, Wind Direction in Degrees Finally, PA is used for unified soil conversion, which solely concerns volumetric water content. The data's serial number is stored in this column. Product name, creation time, units, source, missing data, end of record identifier, and time range are all included in the header.

Table 4.3 shows typical measured data from the WASCAL facility.

| TIMESTAMP TS | CR299SWASCAL RECORD RN | Amount of Rainfall (mm) | Rain rate (mm/hr) |
|------------------|------------------------|-------------------------|-------------------|
| 10/24/2014 0:00 | 4302 | 0 | 0 |
| 10/24/2014 1:00 | 4303 | 5 | 5 |
| 10/24/2014 2:00 | 4304 | 0.8 | 0.8 |
| 10/24/2014 3:00 | 4305 | 0 | 0 |
| 10/24/2014 4:00 | 4306 | 0 | 0 |
| 10/24/2014 5:00 | 4307 | 0 | 0 |
| 10/24/2014 6:00 | 4308 | 0 | 0 |
| 10/24/2014 7:00 | 4309 | 0 | 0 |
| 10/24/2014 8:00 | 4310 | 0 | 0 |
| 10/24/2014 9:00 | 4311 | 0 | 0 |
| 10/24/2014 10:00 | 4312 | 0 | 0 |
| 10/24/2014 11:00 | 4313 | 0 | 0 |
| 10/24/2014 12:00 | 4314 | 0 | 0 |
| 10/24/2014 13:00 | 4315 | 0 | 0 |
| 10/24/2014 14:00 | 4316 | 0 | 0 |
| 10/24/2014 15:00 | 4317 | 0 | 0 |

| | | | | |
|------------|-------|------|---|---|
| 10/24/2014 | 16:00 | 4318 | 0 | 0 |
| 1/8/2014 | 17:00 | 4319 | 0 | 0 |

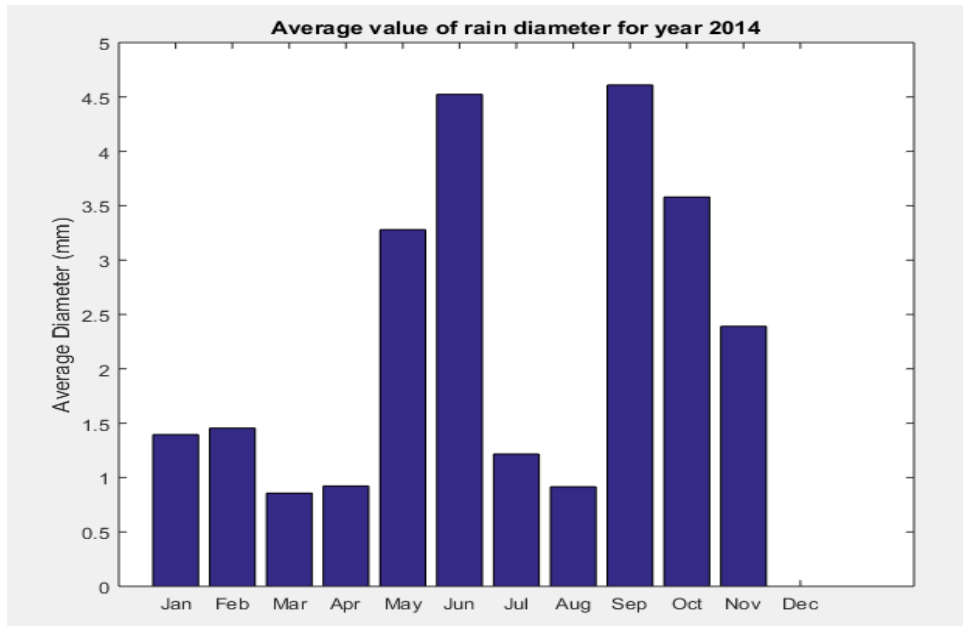


Figure 4.2: Month-by-month average rain diameter chart

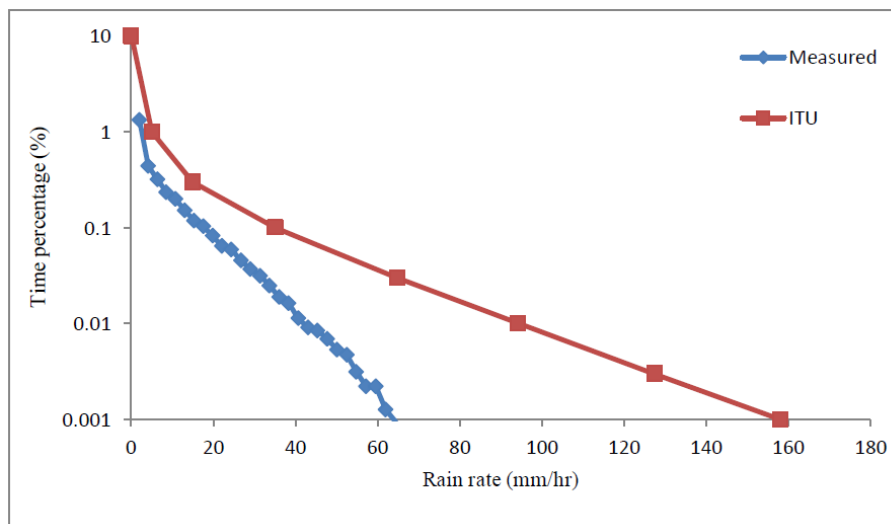


Figure 4.4: Rain rate cumulative distribution at the TRODAN garden site

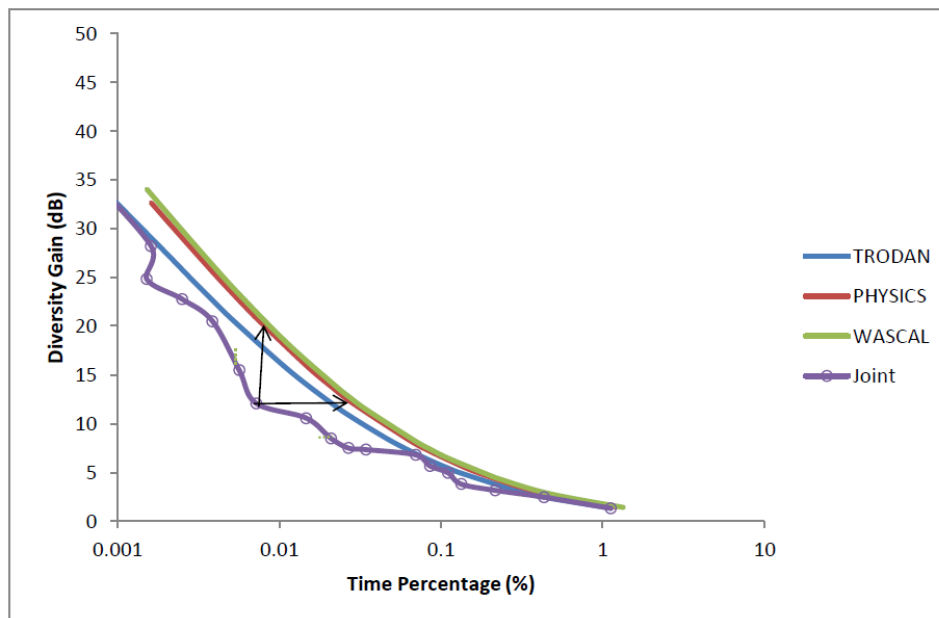


Figure 4.8: At 12 GHz, the cumulative distribution of rain-induced attenuation.

Figure 4.2 shows that rain fade is mostly determined by the rain cell diameter, or the size of the rain cell at the time of rain. The translated rainfall rate is estimated to be around 36 mm/h for 0.01 percent of the time, while the corresponding estimate for the same time percentage is around 94 mm/hr for the ITU-R model. In figure 4.4, this results in a relative inaccuracy of around 20%. Figure 4.8 depicts the Cumulative Distribution Function (CDF) of rain attenuation after selection integrating diversity for the two sites. The TRODAN garden had the lowest monthly precipitation of 85 mm among the three sites, with an improvement factor of 0.02 for 10.5 dB attenuation using TRODAN as the reference site.

IV. CONCLUSION

This study looked into the impact of the rain cell size distribution pattern on signal transmission in the tropical region. Rain data from three different rain locations (A, B, C) were archived for two years between 2012 and 2014 within a system that covered the study of raindrop cell size and its effect on signal propagation at the referenced band for the estimation of site diversity and improvement factor needed to evaluate the size of the rain cell pattern.

REFERENCES

- [1]. **Ajayi, G. O.** (1996). 'Handbook on Radio Propagation related to Satellite Communication in Tropical and Subtropical Countries'. Trieste, Italy, URSI Standing committee on Developing countries and International center for Theoretical Physics.
- [2]. **Arbesser-Rastburg, B.R. and G. Brussaard.** (1993): Propagation research in Europe using the **OLYMPUS satellite**. *Proc. IEEE*, **81**, 865–875.
- [3]. **Awaka, J.** (1989). 'A Three Dimensional Rain cell Models for the Study of Interference due to Hydrometeor Scattering'. *Communications Research Laboratory*, 36(147), pp. 13-44
- [4]. **Emiliani, L. and Lorenzo, L.** (2010). 'Evaluation of Model for the Conversion of T-min Rainfall Distribution to an Equivalent One-Minute Distribution for Colombia'. *Radio Science*, Vol. 8, No. 4, p. 56.
- [5]. **Lee, Y. H, Koh, W. S; Lee, Y. S, and Michelle, H. M.** (2009). 'Overcoming the Rain Fade obstacle, Understanding Singapore's Rain Dynamics and Feasible counter Measurement against Rain fading.
- [6]. **Ojo, J. S., Ajewole, M. O. and Sarkar, S. K.** (2008). 'Rain Rate and Rain Attenuation Prediction for Satellite Communication in Ku and Ka Bands over Nigeria'. *Electromagnetics Research* Vol 5, pp. 207-223.
- [7]. **Omolawi, P. A.** (2011). 'Derivation of One-minute rain rate from five minutes equivalent in South Africa'. *Prog., Electromagnetic Resources* 7(6), pp. 524-535.
- [8]. **Omotosho, T. V. and Oluwafemi C. O.** (2009). 'Impairment of Radio Wave Signal by Rainfall on Fixed satellite service on Earth-space path at 37 Stations in Nigeria'. *Journal of Atmospheric and Solar-Terrestrial Physics*, Vol 71, pp. 830-840.
- [9]. **Omotosho, T. V. Mandeep, J. S and Mardina, A.** (2013). 'Impact of cloud on fixed Satellite Communication Links on Earth-Space path at Ka and V-band in the African Countries'. *International Journal of Engineering and Technology* 3(1) Pp. 830-840.
- [10]. **Palmer, J.** (2014). *Satellite Podcast*.
- [11]. **Pan, Q. W., Allnutt, J. E., and Tsui, C.,** (2001). 'Evaluation of diversity and power control techniques for satellite communication systems in tropical and equatorial rain climates'. *IEEE Trans. Antennas Propagation*, 56, 3293–3301.
- [12]. **Pan, Q. W. and Allnutt, J. E.** (2004). '12 - GHz Fade Durations and intervals in the Tropics'. *IEEE Trans. Antennas and Propagation*, 52, 693–701.
- [13]. **Stallins, W.** (2007). *Data and Computer Communications*. Upper Saddle River, New Jersey, United States, Pearson prentice hall.